UDC 531.391:681.2.08
Original scientific paper
Received: 17.07.2006.

Active vibration control using Terfenol-D with H-infinity filter

Dibakar Bandopadhya, Ashish Dutta and **Bishakh Bhattacharya**
Department of Mechanical Engineering, Indian Institute of Technology, Kanpur, INDIA
e-mails: dibakarb@iitk.ac.in, adutta@iitk.ac.in, bishakh@iitk.ac.in

SUMMARY

In this paper a magnetostrictive material (Terfenol-D) based active vibration control of high amplitude has been proposed. A single link planar flexible manipulator with rotary joint has been modelled using Terfenol-D as smart active material. H-infinity filter is used in the context to estimate the tip deflection (position) and deflection rate (velocity) of the flexible manipulator based on which comparison is made with the active control scheme to compare the performance efficiency. Modal approach is followed for derivation of the dynamic model and then proportional damping scheme is introduced taking account of the properties of the host layer and smart layer. Fabrication of Terfenol-D based composite actuator is also discussed which is used in the experiment. Simulations are first performed to demonstrate effective vibration containment and the results proved that the proposed method could attenuate vibration effectively. However, to identify the elastic displacements as generalized coordinates an optimal performance is required. This is carried out by discretization of the elastic motion through the assumed mode technique and applying H-infinity filter. H-infinity filter is used to compare the active vibration control performance with the damping scheme. Experiments are conducted to verify the simulation results.

***Key words**: modal frequency, smart composite actuator, proportional damping, H-infinity filter, Terfenol-D.*

1. INTRODUCTION

A flexible manipulator being a continuous dynamics system has infinite degrees of freedom and is governed by the coupled-nonlinear partial differential equations. Finding the closed form solution for response of such a system is extremely difficult, particularly as we move onto multilink cases [1-2].

Besides these other practical constraints like finite dimensional actuators and sensors make it necessary to discretize the system while finding the system dynamic equation. In finite element method flexible link is considered as an assembly of finite number of elements, where each element satisfies the required continuity and convergence condition [3]. Owing to simplicity of the shape functions, which are local in nature, less number of mathematical operations is required for inertia matrix computation as compared to that in case of assumed mode technique [4]. Various passive damping, active damping and combined damping schemes have been proposed in the past to restrain such vibration within desired limit. Smart piezoelectric materials have been used successfully for controlling vibration of a single and a two link planar link [5-10]. With the development of composite materials, manipulator made of composite laminates exhibit non-proportional damping. To avoid the above stated problem a hybrid damping scheme is proposed [11]. During vibration, the coating of such smart materials undergoes a change of strain, initiates a movement of magnetic domains thereby dissipates the mechanical energy through hysteresis [12-14]. However, the hybrid damping scheme is difficult to use for flexible manipulator due to complex non-linear

equation of motion. To meet the requirements for pointing accuracy, flexible body parameters such as elastic displacement are of great importance for control tasks and should be continuously identified in the working environment. Using the well-known H-infinity filter algorithm the identification of flexible body parameters is found to be more efficient in the present study [15-19].

In this study Hamiltonian approach is used for derivation of the dynamic model of the rotating flexible link. First, the total kinetic and potential energies are obtained for the link in-terms of flexible degrees of freedom and joint variables. Smart materials as actuators bonded to the surface of the flexible manipulator are used to repress the link vibration. Proportional damping scheme is introduced next in modelling as it is quite straight forward to incorporate into the model to illustrate the efficiency of vibration control using smart materials with the estimation algorithm. H-infinity filter gives the smallest possible estimation error by minimizing the ∞-norm of the estimation error where the expected value of estimate is equal to the true state on an average. H-infinity filter minimizes the worst case estimation error. This is actually minimizing the maximum singular value of the transfer function from the noise to the estimation error. The main objectives of this paper are:

a. To introduce smart active damping scheme using active smart magnetostrictive material Terfenol-D;
b. To estimate the tip deflection and deflection rate of the flexible link using the well known H-infinity filter;
c. To compare the performance of the active damping scheme with the estimation algorithm.

The proposed method explores electro/magneto-mechanical coupling under a control voltage/magnetic flux. The smart material bonded to the flexible structure generates an end moment that opposes the structural deformation under the control voltage. In current work, a strain dependent active damping is proposed. It has been found that ceramic and ferromagnetic coatings yields significant damping over a wide range of frequency. However, for structural vibration control induced strains are often at least one order higher in magnitude. Hence if only ferromagnetic material is used the extent of damping achieved may be negligible. Smart magnetostrictive material like the Terfenol-D is used to achieve active damping in the manipulator. Such material can be used as an intelligent distributed layer over the link to introduce distributed control vibration. A series of closely packed coils enclose the magnetostrictive patch along the link length and by driving the required current, a distributed active strain is generated in the magnetostrictive layer which opposes the structural deformation. In comparison with the mostly used smart materials PZT magnetostrictive material like Terfenol-D possesses certain advantages. Magnetostrictive materials can operate at higher temperatures than piezoelectric and electrostricive actuators. They can undergo higher strains and require lower input voltages. Degraded PZT requires repoling. Magnetostriction of aligned Terfenol-D does not require demagnetization however PZT has higher bandwidth but low fatigue life.

In section 2 dynamic model of the flexible link is derived using modal approach. Section 3 deals with the damping scheme and fabrication of Terfenol-D based composite actuator. H-infinity filter is discussed in Section 4. Section 5 presents simulation results while Section 6 discusses the experiment results. Finally, conclusions are drawn in Section 7.

2. DYNAMIC MODEL DERIVATION USING MODAL APPROACH

The dynamic model of the system is derived following the assumed mode method integrated with the smart actuator dynamic. In assumed mode method the elastic deflection $\varphi(x,t)$ is represented as:

$$\varphi(x,t) = \sum_{i=1}^{n} \eta_i(t)\,\psi_i(x) \qquad (1)$$

where, $\psi_i(x)$ are the mode shapes of the flexible link and $\eta_i(t)$ are the time dependent flexible body coordinates. It is assumed that the link has planar motion and vibrates in the horizontal direction. The shear deformation and rotary inertia are ignored for simplicity.

2.1 Kinetic energy of the system

The total kinetic energy of the system is the sum of the kinetic energy of the flexible manipulator and kinetic energy of the payload as shown in Figure 1. Since the velocities at each point on the link depends on the position and time, kinetic energy of the link at any time is an integral over the length of the link.

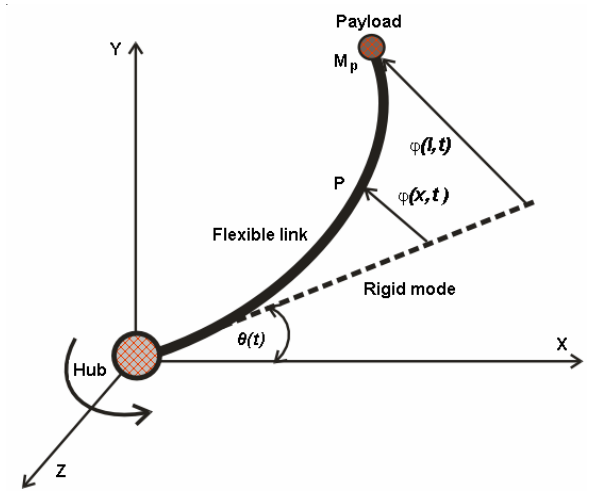

Fig. 1 Flexible manipulator configuration

Position vector of any point $P(x)$ on the link is given by:

$$P(x)=\begin{bmatrix} x\cos(\theta)-\varphi(x,t)\sin(\theta) \\ x\sin(\theta)+\varphi(x,t)\cos(\theta) \end{bmatrix} \quad (2)$$

where, θ= Hub angle with respect to the inertial X-axis and $\varphi(x,t)=\psi(x)\eta(x)$ in time and space. Mode shape is given by:

$$\psi(x)=A_1\sin(\beta x)+A_2\cos(\beta x)+ \\ +A_3\sin(h\beta x)+A_4\cos(h\beta x) \quad (3)$$

where, the constant coefficients A_1, A_2, A_3, A_4 and the parameter β are to be determined by using boundary conditions considering Euler-Bernoulli beam theory. This gives the characteristic equation of equality:

$$\cos\beta l\cosh\beta l+1=0 \quad (4)$$

The solution of Eq. (4) gives infinite values of βl. The first six values are given by:

$$\left[(\beta l)_i\right]_{i=1}^{i=6}= \\ =\left[1.8751 \quad 4.6941 \quad 7.8548 \quad 10.9955 \quad 14.1372 \quad 17.2788\right]$$

and the corresponding frequencies are given by:

$$\omega_i=\left\{(\beta l)_i\right\}^2\sqrt{\frac{EI}{ml^4}} \quad (5)$$

where, m is the mass per unit length of the link, E is the modulus of elasticity of the link and I is the area moment of inertia. Figure 2 shows the bending moment variation of the flexible link for the first six modes of vibration.

The quantities ω_i $(i=1,2,...,\alpha)$ are called characteristic values or eigenvalues. They are also known as natural frequencies. Therefore, the velocity is obtained as:

$$\dot{P}=\begin{bmatrix} -x\sin(\theta)\dot{\theta}-\dot{\varphi}(x,t)\sin(\theta)-\varphi(x,t)\cos(\theta)\dot{\theta} \\ x\cos(\theta)\dot{\theta}+\dot{\varphi}(x,t)\cos(\theta)-\varphi(x,t)\sin(\theta)\dot{\theta} \end{bmatrix} \quad (6)$$

Thus:

$$\dot{P}.\dot{P}=x^2\dot{\theta}^2+\dot{\varphi}^2+\varphi^2\dot{\theta}^2+2x\dot{\theta}\dot{\varphi} \quad (7)$$

Therefore, the kinetic energy of the link is given by:

$$T_l=\frac{1}{2}m\int_0^l\dot{P}.\dot{P}\,dx= \\ =\frac{m}{2}\frac{l^3}{3}\dot{\theta}^2+\frac{m}{2}\int_0^l\psi(x)^2\dot{\eta}(t)^2\,dx+ \\ +\frac{m}{2}\int_0^l\psi(x)^2\eta(t)^2\,dx+\frac{m}{2}\int_0^l 2x\dot{\theta}\psi(x)\dot{\eta}(t)\,dx \quad (8)$$

And kinetic energy due to payload is:

$$T_p=\frac{1}{2}M_p\left[\dot{P}(l).\dot{P}(l)\right]= \\ =\frac{M_p}{2}\left[l^2\dot{\theta}^2+\dot{\varphi}(l,t)^2+\varphi(l,t)^2\dot{\theta}^2+2l\dot{\theta}\dot{\varphi}(l,t)\right] \quad (9)$$

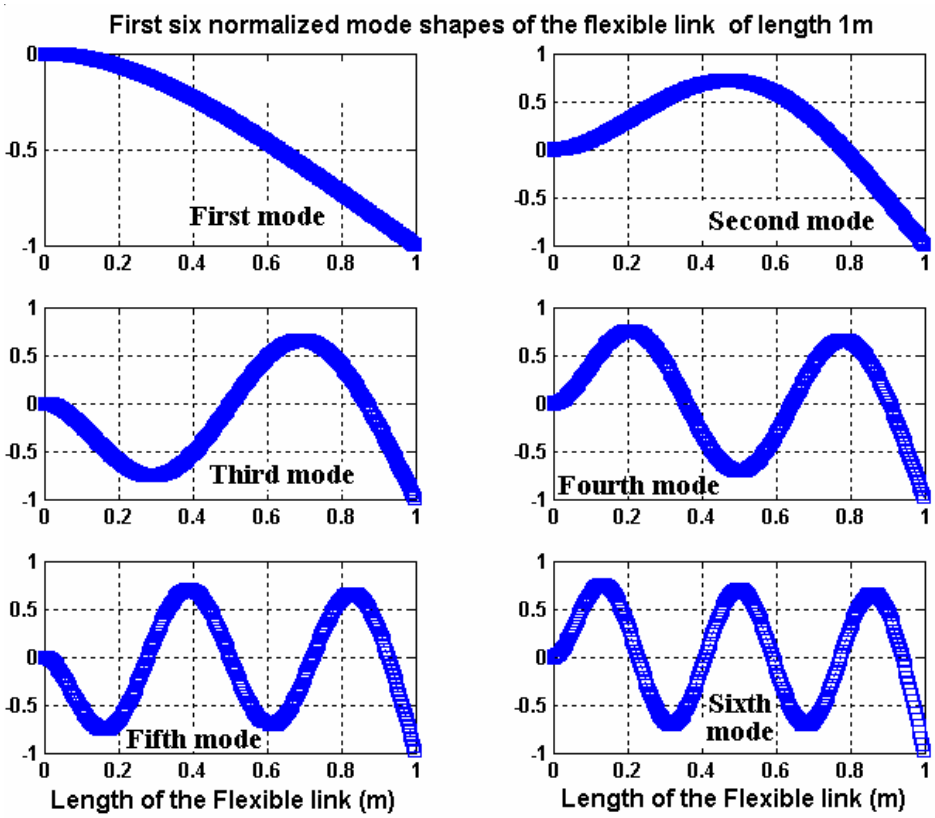

Fig. 2 Bending moment variation for first six modes of the flexible link of length 1 m

Therefore, total kinetic energy is given by:

$$T = T_l + T_p = \frac{m}{2}\frac{l^3}{3}\dot{\theta}^2 + \frac{m}{2}\int_0^l \psi(x)^2 \dot{\eta}(t)^2\,dx + \frac{m}{2}\int_0^l \psi(x)^2 \eta(t)^2\,dx + \frac{m}{2}\int_0^l 2x\dot{\theta}\psi(x)\dot{\eta}(t)\,dx + \frac{M_p}{2}\left[l^2\dot{\theta}^2 + \dot{\varphi}(l,t)^2 + \varphi(l,t)^2\dot{\theta}^2 + 2l\dot{\theta}\dot{\varphi}(l,t)\right] \tag{10}$$

Letting, $M_a = M_p l^2 + \frac{1}{3}ml^3$, $M_b = M_p\psi(l)^2 + \int_0^l m\psi(x)^2\,dx$, $M_c = M_p l\psi(l) + \int_0^l mx\psi(x)\,dx$

Therefore, total kinetic energy is obtained as taking account of M_b as symmetric matrix:

$$T = \frac{M_a}{2}\dot{\theta}^2 + \frac{1}{2}\eta^T M_b \eta\dot{\theta}^2 + \frac{1}{2}\dot{\eta}^T M_b\dot{\eta} + M_c\dot{\eta}\dot{\theta} \tag{11}$$

2.2 Potential energy

Potential energy of the system is due to deformation of the link and it depends on position of the link and time. Hence the potential energy of the link is given by:

$$V_p = \frac{1}{2}\int_0^l EI\left(\varphi''(x,t)\right)^2 dx \tag{12}$$

On simplification:

$$V_p = \frac{1}{2}\eta^T K\eta \tag{13}$$

where $K(i,j) = \frac{1}{2}\int_0^l EI\psi''_i(x)\psi''_j(x)\,dx$. Since the payload is considered as a point mass and the rotation is in a plane normal to gravity hence there is no potential energy due to payload.

2.3 Work done due to input torque and smart patches

The virtual work done by input torque $T(t)$ acting on the hub and each actuator can be expressed as:

$$\delta W = T(t)\delta\theta + \int_{x_1}^{x_2}\tau_i(x,t)\frac{bt_b}{2}\left(\delta\theta + \psi'(x)\delta\eta\right)dx \tag{14}$$

where x_1 and x_2 indicates the co-ordinates along the link length. Assume that patch length and width remains constant. Using 'n' number of patches, the virtual work by all the patches may be expressed as:

$$\delta W = \sum_{i=1}^{n}\delta W_i = T(t)\delta\theta + \sum_{i=1}^{n}\tau_i(t)\delta\theta + \sum_{i=1}^{n}\tau_i(t)\left[\psi'(x_{i+1}) - \psi'(x)_i\right]\delta\eta \tag{15}$$

where $\tau_i(t)$ is the bending moment generated by the smart active layer. The term $\left[\psi'(x_{i+1}) - \psi'(x_i)\right]\delta\eta$ denotes the slope difference between two ends of the *i-th* actuator (patch). Further, assuming that bending moment generated for each patch is equal then the above equation will be simplified to:

$$\delta W = T(t)\delta\theta + \tau(t)\delta\theta + \tau(t)\left[\psi'(u_2) - \psi'(u_1)\right]\delta\eta \tag{16}$$

where $(u_2–u_1)$ is the smart patch coverage and $\tau(t)$ is the total bending moment.

2.4 Equation of motion

After finding the total kinetic and potential energy, the final equation of motion is obtained by applying the Hamiltonian principle:

$$\int_{t_0}^{t_f}\left(\delta T - \delta V_p + \delta W\right)dt = 0 \tag{17}$$

Therefore, Eq. (17) is transformed into:

$$\int_{t_0}^{t_f}\Big(M_a\dot{\theta}\delta\dot{\theta} + M_b\eta\delta\eta\dot{\theta}^2 + \eta^T M_b\eta\dot{\theta}\delta\dot{\theta} + M_c\delta\dot{\eta}\dot{\theta} + M_c\dot{\eta}\delta\dot{\theta} + M_b\dot{\eta}\delta\dot{\eta} - \eta^T K\delta\eta + T(t)\delta\theta + \tau(t)\delta\theta + \tau(t)\left[\psi'(u_2) - \psi'(u_1)\right]\delta\eta\Big)dt = 0 \tag{18}$$

Since variation of θ i.e. $\delta\theta(t_0)=\delta\theta(t_f)=0$ and $\delta\eta(t_0)=\delta\eta(t_f)=0$. Thus after integration Hamiltonian is reduced to:

$$\int_{t_0}^{t_f}\Big[-\left(M_a\ddot{\theta} + 2M_b\dot{\eta}\dot{\theta} + \eta^T M_b\eta\ddot{\theta} + M_c\ddot{\eta}\right)\delta\theta - \left(M_c\ddot{\theta} + M_b\ddot{\eta}\right)\delta\eta + M_b\eta\delta\eta\dot{\theta}^2 - \eta^T K\delta\eta + T(t)\delta\theta + \tau(t)\delta\theta\Big]dt$$

Now clubbing the terms contains $\delta\theta$ and $\delta\eta$, further because the virtual quantities $\delta\theta$ and $\delta\eta$ are arbitrary. Therefore, the coefficients associated with them must vanish to make:

$$M_a\ddot{\theta} + \eta^T M_b\eta\ddot{\theta} + M_c\ddot{\eta} + 2M_b\dot{\eta} = T(t) + \tau(t) \tag{19}$$

$$M_c\ddot{\theta} + M_b\ddot{\eta} + K\eta - M_b\eta\dot{\theta}^2 = 0 \tag{20}$$

Both equations can now be written in matrix form:

$$\begin{bmatrix} M_a+\eta^T M_b\eta & M_c \\ M_c & M_b \end{bmatrix}\begin{bmatrix} \ddot{\theta} \\ \ddot{\eta} \end{bmatrix}+\begin{bmatrix} M_b\dot{\eta} & M_b\dot{\theta} \\ -M_b\eta\dot{\theta} & 0 \end{bmatrix}\begin{bmatrix} \dot{\theta} \\ \dot{\eta} \end{bmatrix}+\begin{bmatrix} 0 \\ K\eta \end{bmatrix}=\begin{bmatrix} T(t)+\tau(t) \\ 0 \end{bmatrix} \tag{21}$$

3. DAMPING SCHEME

In a flexible manipulator system, damping is present in several possible forms. In structural damping due to the flexibility of manipulator arm, energy is dissipated within the arm material that leads to structural damping. In Figure 3 it is shown that the first three modes take the maximum energy and on increment of mode numbers, total energy does not change appreciably. Based on this we have taken three patches of Terfenol-D based composite actuator to suppress the three major modes of vibration.

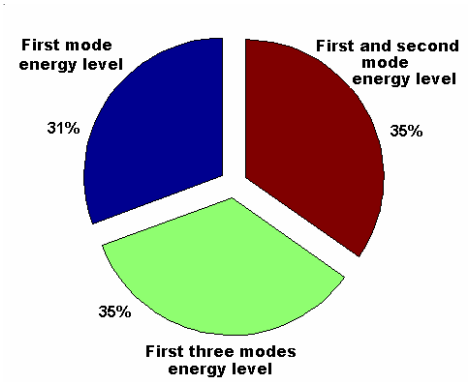

Fig. 3 Normalized energy level ratio for the first three modes of the flexible manipulator

The positions of the three patches of Terfenol-D composite have been located on the link considering first three mode shapes of the flexible manipulator as shown in Figure 4.

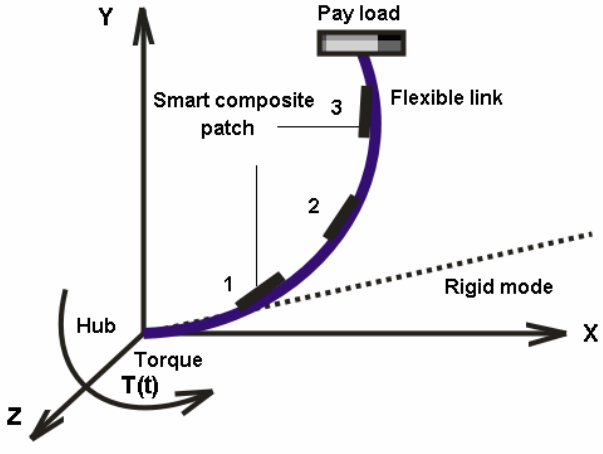

Fig. 4 Flexible manipulator with three smart patches as actuators

Proportional damping matrix can be found from the following relationship:

$$\boldsymbol{C}=\boldsymbol{AM}+\boldsymbol{BK} \tag{22}$$

where, the constants $\boldsymbol{A}$ and $\boldsymbol{B}$ are given by:

$$\boldsymbol{A}=\frac{2\omega_{n_1}\omega_{n_2}\left(\omega_{n_2}\xi_1-\omega_{n_1}\xi_2\right)}{\omega_{n_2}^2-\omega_{n_1}^2} \tag{23}$$

$$\boldsymbol{B}=\frac{2\left(\omega_{n_2}\xi_2-\omega_{n_1}\xi_1\right)}{\omega_{n_2}^2-\omega_{n_1}^2} \tag{24}$$

where ω_{n1} and ω_{n2} are the first and second undamped natural frequencies, and ξ_1 and ξ_2 are the respective damping factors. The damping factors are determined experimentally by measuring the decrement in the link vibrations. However, this method does not take into account the joint and actuator friction. After finding the damping matrix $\boldsymbol{C}$ the modified equation of motion for a damped system is written as:

$$\boldsymbol{M}\ddot{q}+\boldsymbol{C}\dot{q}+f(q,\dot{q})+\boldsymbol{K}q=Q_r \tag{25}$$

where $\boldsymbol{M}$ is the mass matrix, $\boldsymbol{C}$ is the damping matrix, f is the non-linear coupling term, $\boldsymbol{K}$ is the stiffness matrix and $\boldsymbol{Q}_r$ is the right hand side force term.

3.1 Fabrication of Terfenol-D based actuator

Fabrication of Terfenol-D based composite actuator has been reported in details [13] following the standard literature [20]. Terfenol-D powder and epoxy are homogeneously mixed up in the proportion of *60 %* (*15 gm*) and *40 %* (*10 gm*) and then put it in a mould of size *7.5 cm x 4 cm x 0.15 cm* after eliminating the air bubbles by keeping it into vacuum for *30* minutes. The mould is then placed between a pair of strong permanent magnets. The uniform magnetic field in longitudinal direction makes the particles to align with the magnetic flux lines. The whole arrangement as shown in Figure 5 is then kept in an oven maintained at *70°C* for *8* hours to ascertain the full cure of the composites. The cured composite is then cut into pieces as patches according to the requirement.

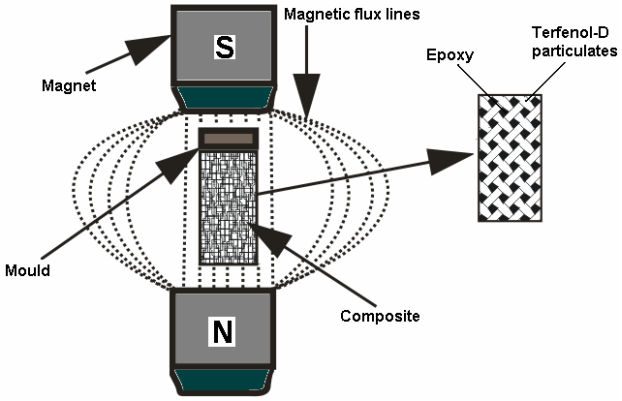

Fig. 5 Arrangement for fabrication process

4. H-INFINITY FILTER

In this section H-infinity filter is used to estimate the system parameters and then comparison is made with the active damping scheme. The H-infinity filter is a computational algorithm containing a sequence of time and measurement updating of the estimates of the system. It is used to identify the elastic displacements or system identification parameters. The filter can incorporate dynamic noise in the dynamical model of the state. It is a real time estimator supplying the estimates for the instant that the measurement is available. The filter consists of two cycles:

* Time Update,
* Measurement Update.

4.1 State dynamics model

Let state dynamical model may be represented as:

$$\dot{x} = \boldsymbol{A}x + \boldsymbol{B}u + v \tag{26}$$

where, $x = \begin{pmatrix} \theta & q & \dot{\theta} & \dot{q} \end{pmatrix}$ is the state continuously variant with the time, $\boldsymbol{B}$ is the input matrix in addition of process noise v and $\boldsymbol{A}$ is system matrix that relates the state timely and linearly, given by:

$$\boldsymbol{A} = \left[\begin{array}{c|c} \boldsymbol{0} & \boldsymbol{I} \\ \hline -\bar{\boldsymbol{K}} & -\bar{\boldsymbol{C}} \end{array}\right]$$

where, $\bar{\boldsymbol{K}} = diag\left\{0, \quad \omega^2\right\}$, the matrix contains the squared natural frequencies, and the damping matrix $\bar{C} = \{0, \quad 2\xi\omega\}$.

4.2 Measurement model

The measurement model is given by:

$$\boldsymbol{y} = \boldsymbol{H}x + v \tag{27}$$

where $\boldsymbol{y}$ is the measurement vector composed by the angle θ and $\dot{\theta}$ angular velocity observables. The measurements of θ and $\dot{\theta}$ are taken by position and velocity sensor. For the angular position and velocity it is assumed nominally a standard deviation of *0.1°* and *0.01°/s* respectively. The $\boldsymbol{H}$ matrix relates the measurements to the state by:

$$\boldsymbol{H} = \begin{bmatrix} 1 & 0 & 0 & 0 \\ 0 & 0 & 1 & 0 \end{bmatrix} \tag{28}$$

and v represents the measurement noise. The specific equations for the time and measurement updates are presented below. The estimator structure is assumed to be in the following predictor – corrector form:

$$\hat{x}_{k+1} = A\hat{x}_k + K_k\left(y_{k+1} - HA\hat{x}_k\right) \tag{29}$$

where K_k is some gain which we need to determine. Simultaneous equation solved for the gain K_k and is given by:

$$K_k = \left(I + \frac{P}{\gamma^2}\right)^{-1} PH^T \tag{30}$$

$$M = APA^T + I \tag{31}$$

$$P^{-1} = M^{-1} - I/\gamma^2 + H^T H \tag{32}$$

Here objective is to find filter gain K_k such that the maximum singular value is less than γ. Posible situations are: (i) $\hat{x}_k \in R^n$: Priori state estimate at step k; (ii) $\hat{x}_{k+1} \in R^n$: Posteriori state estimate at step k; (iii) $P \in R^n$: Priori estimate error covariance at step k; (iv) $y_{k+1} - HA\hat{x}_k$: The measurement innovation or residual. The first task during the measurement update is to compute the H-infinity gain K_k. After each time and measurement update pair, the process is repeated with the previous posteriori estimates used to project or predict the new a priori estimates.

5. SIMULATION RESULTS

In this section, we discuss the results obtained from numerical simulation of single-link flexible manipulator. All programs are developed in MATLAB using the material properties and parameters given in Tables 1 and 2. To solve the differential equations in state space, an in-built function of MATLAB called "ode45" is used which is based on 4^{th} and 5^{th} order Runga-Kutta scheme with adaptive step size [14].

5.1 Properties of different materials

Table 1. Physical properties of host and smart layers

Magnetostrictive Layer (Terfenol-D)	
Magneto-mechanic constant (d)	1.67×10^{-8} *m/A*$^{-1}$
Coil radius (r_c)	*0.8 m*
Gain (k_1)	*0.7*
Number of coils (n)	*3*
Coil constant ©	*3.1235*
Host Layer Aluminum	
Moment of inertia (I)	7.2×10^{-9} *m*^{4}
Mass per unit length (m)	*4.93 Kg/m*
Length of link (L)	*1 m*
Width of link (w)	*50 mm*
Thickness (t)	*10 mm*

Table 2. Other parameters used in simulation

Parameters	*Aluminum (Al)*	*Terfenol-D*
Elastic Modulus (E)	*70 GPa*	*26.5 GPa*
Density (ρ)	*2700 Kg/m^3*	*9250 Kg/m^3*
*Coefficient (**A**)*	*0.0273*	
*Coefficient (**B**)*	*0.0017*	
First fundamental frequency (ω_{n1})	*1.5829 (rad/sec)*	
Second modal frequency (ω_{n2})	*9.92 (rad/sec)*	
Damping coefficient (ξ_1&ξ_2)	*0.01*	

5.2 Proportional damping

Firstly the response of an undamped and damped single link manipulator of very small thickness under a sinusoidal input torque of magnitude *1 Nm* is shown. It is observed that the smart proportional damping is able to attenuate the link vibrations effectively and the result obtained validates the experiment results. In all the result presented above the damping of joint angular motion is considered. Figures 6 and 7 are showing the undamped and damped response of the flexible link with smart proportional damping scheme, while Figure 8 is showing the undamped and damped response of the flexible link and Figure 9 shows the percentage of reduction in tip deflection. It is observed that active proportional damping scheme is able to reduce the vibration up to *65-70 %*.

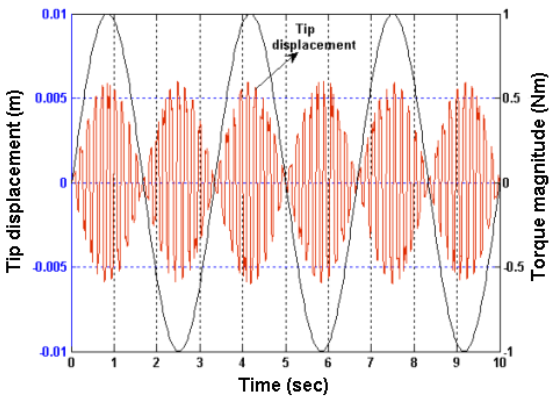

Fig. 6 Undamped response of the flexible link for sinusoidal torque input

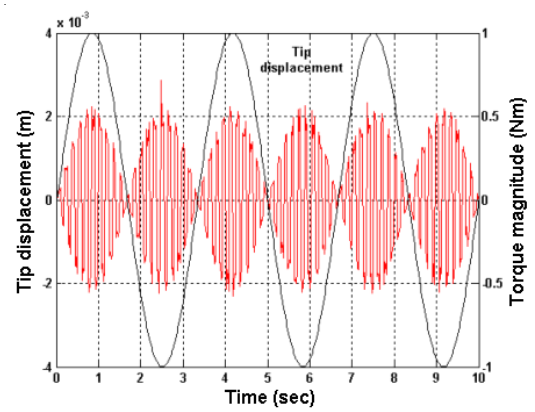

Fig. 7 Damped response of the flexible link for sinusoidal torque input

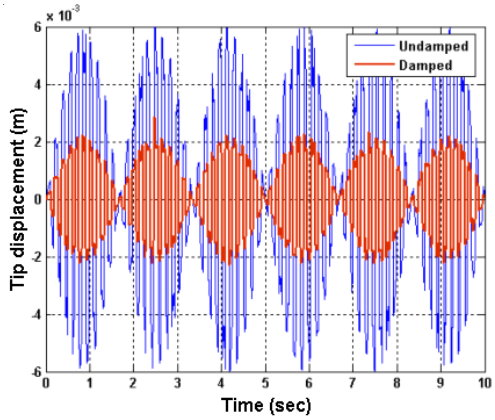

Fig. 8 Undamped and damped response of the flexible link for sinusoidal torque input

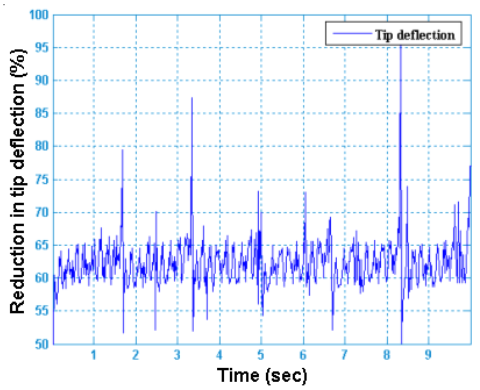

Fig. 9 Reduction of the tip deflection for sinusoidal torque input

5.3 H-infinity filter

In this section H-infinity filter estimates the position and angular velocity of the link under sinusoidal torque input. Filter's performance is assessed for a time step of 2500 while total time is taken 1 sec to estimate the system variables. Figures 10 and 11 shows the true position i.e. tip deflection and velocity i.e. deflection rate of the link about its mean axis while Figures 12 and 13 are showing the estimated deflection and deflection rate using the filter and it is found that relative error of estimation is *7.73%* and *7.42%* respectively.

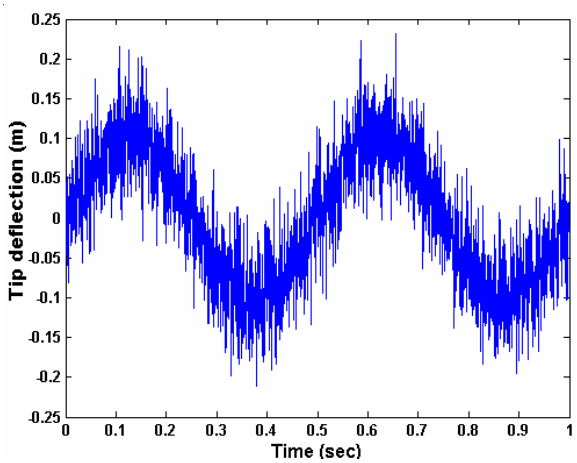

Fig. 10 True position of the link about mean axis

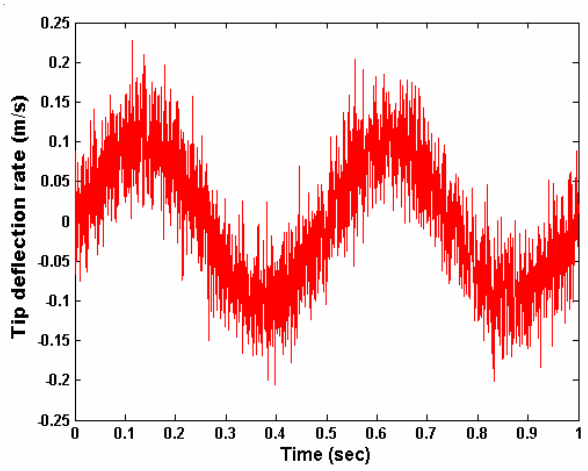

Fig. 11 True velocity of the link about mean axis

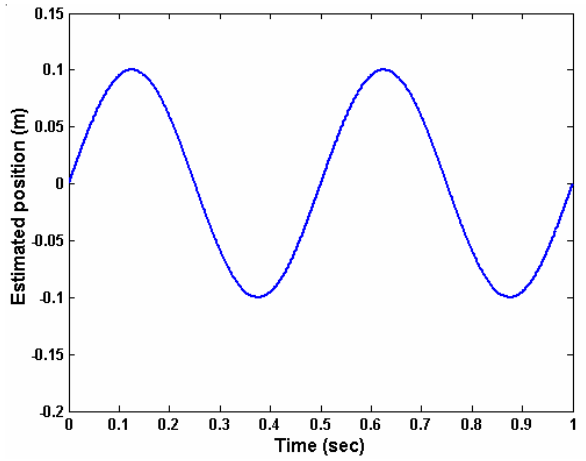

Fig. 12 Estimated position using H-infinity filter

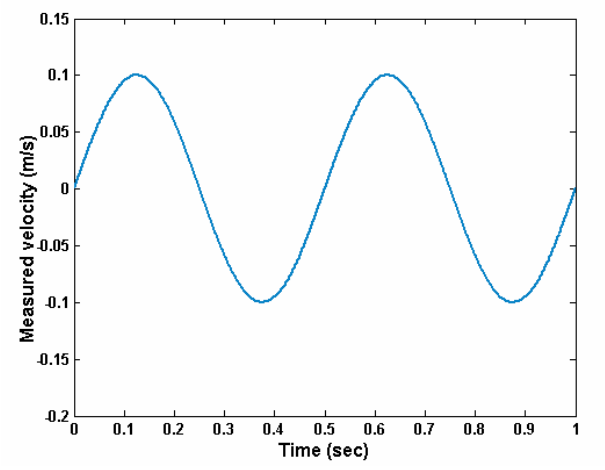

Fig. 13 Estimated velocity using H-infinity filter

Figure 14 shows the filter performance to estimate the tip deflection and deflection rate while Figures 15 and 16 shows the measured tip deflection and deflection rate.

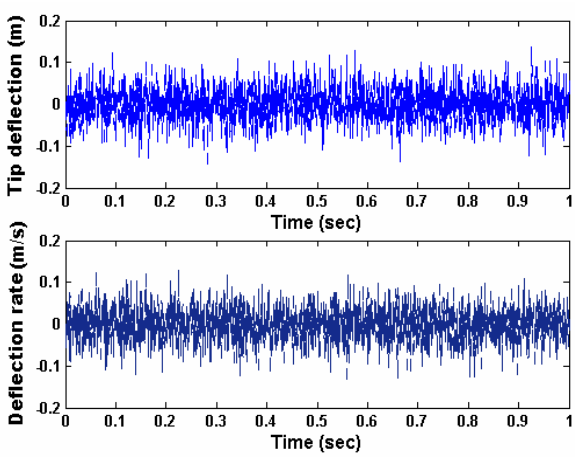

Fig. 14 Estimated tip deflection and deflection rate error in H-infinity filter

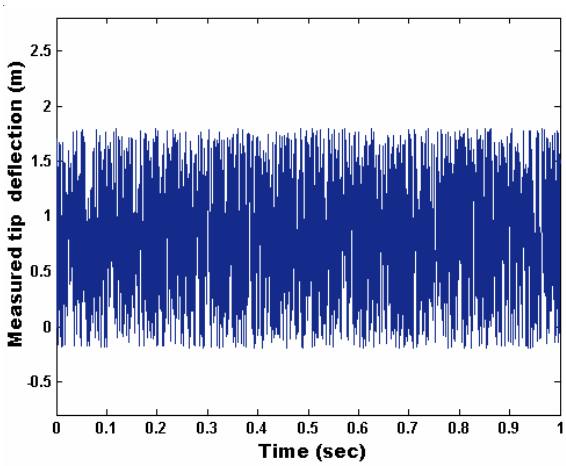

Fig. 15 Measured tip deflection using H-infinity filter

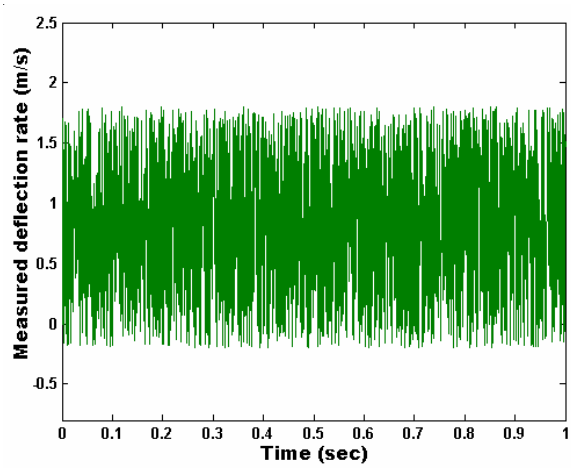

Fig. 16 Measured tip deflection rate using H-infinity filter

6. EXPERIMENT RESULTS

In the experiment setup as shown in Figure 17 aluminum made flexible link is tested. Strain gauge is mounted at the base of the specimen's fixed end. DAQ-PCI-6251, NI-DAQmx devices (supplied by National Instrumentation) with signal conditioner configurable connectors is used for data acquisition. Strain gauge is connected in a quarter bridge mode, resistance of strain gauge bonded on the flexible link is *120 Ω* with gauge factor of *2.11*.

Specifications:

Amplifier gain: *10*
Excitation Voltage Source: *2.5 V*
Excitation Current Drive: *167 mA*
Excitation Sensing: Local sensing
Strain Gauge:
Gauge Type: BFLA-2-8
Gauge Factor: *2.11*
Adhesive: *NP-50*
Gauge Resistance: *120 Ω*
Coefficient of thermal expansion: *8.1e-6/deg-c*
Temperature Coefficient of G.F: *+.12+.05(%)10deg-c*

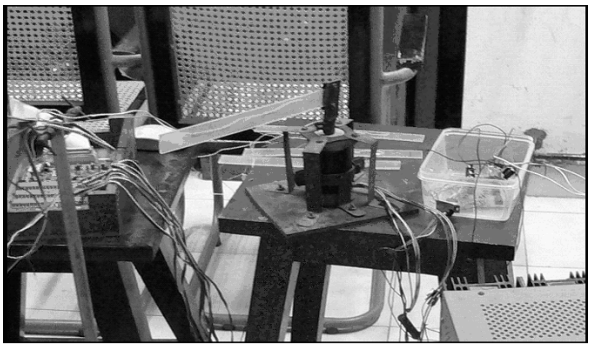

Fig. 17 Experiment setup is used for the damping scheme

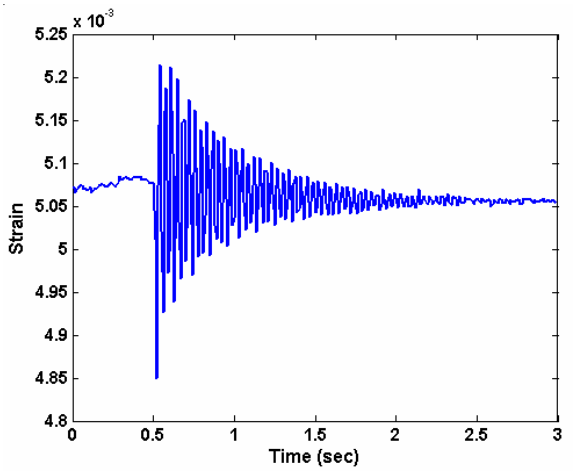

Fig. 18 Damped vibration response for an initial displacement of 8 mm

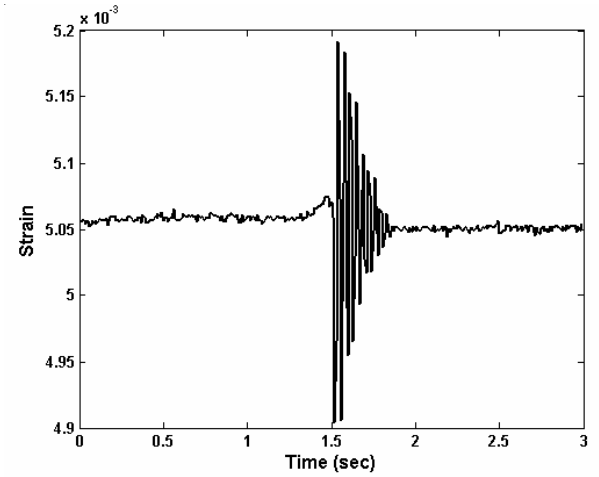

Fig. 19 Damped vibration response for an impact force of 0.098 N

Figures 18 and 19 are showing the strains gradually reducing as damping increased, for initial deflection with impact disturbance. To know the reliability of data, we have also used another piezoelectric (bimorph) sensor. Sensor data acquisition is done through Picoscope interfaced with a PC. Figures 20 and 21 show the undamped and damped response for the sinusoidal input disturbance.

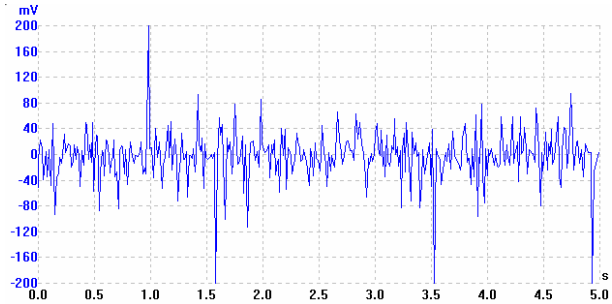

Fig. 20 Undamped vibration response of the flexible link for sinusoidal input disturbance

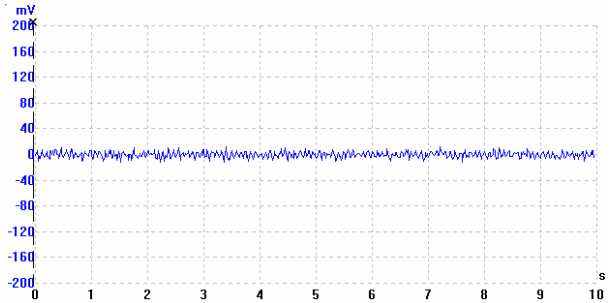

Fig. 21 Damped vibration response for sinusoidal input disturbance

From Figures 18 up to 21, it is observed that around *60-70%* reduction of vibration as tip deflection could be achieved by using three patches of Terfenol-D based composite actuator.

7. CONCLUSION

The main contributions of the paper are that it has been proved both analytically and experimentally that smart magnetostrictive materials based active vibration control scheme can effectively attenuate vibration in flexible rotating link and also vibrating flexible structure under vibration. H-infinity filter algorithm is found fruitful to estimate the position and velocity of the link and based on which comparison is made with the smart damping scheme. It is observed that incrementing smart patches would be a good means to attenuate the high amplitude vibration. This would of course increase the cost of control.

8. REFERENCES

[1] B. Subudhi and A.S. Morris, Dynamic modeling, simulation and control of a manipulator with flexible links and joints, *Robotics and Autonomous Systems*, Vol. 41, pp. 257-270, 2002.

[2] S.M. Yang, J.A. Jenh and Y.C. Liu, Controller design of a distributed slewing flexible structure - A frequency domain approach, *ASME J. Dynam. Syst. Measurement Control*, Vol. 119, pp. 809-814, 1997.

[3] R.J. Theodore, Dynamic modeling and control analysis of multilink flexible manipulator, Ph.D. Thesis, Department of Mechanical Engineering, Indian Institute of Science, Bangalore, 1995.

[4] J. Petrić, Mathematical modeling of the flexible one-link manipulator by finite element method, *International Journal for Engineering Modeling*, Vol. 8, No. 3-4, pp. 77-84, 1995.

[5] H.-K. Kim, S.-B. Choi and B.S. Thompson, Compliant control of two-link flexible manipulator featuring piezoelectric actuators, *Mechanism and Machines Theory*, Vol. 36, No. 3, pp. 411-424, 2000.

[6] P.B. Usoro, R. Nadira and S.S. Mahil, A finite element/Lagrangian approach to modelling light weight flexible manipulators, *Trans of ACME - Journal of Dynamic Systems, Measurements and Control*, Vol. 108, No. 3, pp. 198-205, 1986.

[7] H.Ch. Shin and S.B. Choi, Position control of a two-link flexible manipulator featuring piezoelectric actuators and sensors, *Mechatronics*, Vol. 11, No. 6, pp. 707-729, 2001.

[8] H.-K. Kim, S.-B. Choi and B.S. Thompson, Compliant control of two-link flexible manipulator featuring piezoelectric actuators, *Mechanism and Machines Theory*, Vol. 36, No. 3, pp. 411-424, 2000.

[9] H.Ch. Shin and S.B. Choi, Position control of a two link flexible manipulator featuring piezoelectric actuators and sensors, *Mechatronics*, Vol. 11, No. 6, pp. 707-729, 2001.

[10] Dong Sun, J.K. Mills, Jinjun Shan and S.K. Tso, A PZT actuator control of a single-link flexible manipulator based on linear velocity feedback and actuator placement, *Mechatronics*, Vol. 14, No. 4, pp. 381-401, 2004.

[11] B. Bhattacharya, Vibration suppression of smart laminated composite links and plates, Ph.D. Thesis, Department of Aerospace Engineering, Indian Institute of Science, Bangalore, India, 1995.

[12] B. Bhattacharya, B.R. Vidyashankar, S. Patsias and G.R. Tomlinson, Active and passive vibration control of flexible structures using a combination of magnetostrictive and ferromagnetic alloys, Proc. SPIE - Int. Symp. on Applied Photonics, Glasgow, pp. 204-214, 2000.

[13] D. Bandopadhya, B. Bhattacharya and A. Dutta, Modeling of hybrid damping scheme using smart magnetostrictive composites for flexible manipulator, *Journal of Reinforced Plastics and Composites*, Vol. 26, No. 9, pp. 861-880, 2007.

[14] D. Bandopadhya, S.S. Padhe and B. Bhattacharya, Distributed vibration control in flexible manipulator using smart hybrid damping scheme, Proc. of the ICTACEM-2004, IIT Kharagpur, 2004.

[15] D. Simon, A game theory approach to constrained minimax state estimation, *IEEE Transactions on Signal Processing*, Vol. 54, No. 2, pp. 405-412, 2006.

[16] D. Simon and D.L. Simon, Aircraft turbofan engine health estimation using constrained Kalman filtering, *ASME Journal of Engineering for Gas Turbines and Power*, Vol. 127, No. 2, pp. 323-328, 2005.

[17] D. Simon, H. El-Sherief, Hybrid Kalman/minimax miltering in phase locked loops, *Control Engineering Practice*, Vol. 4, No. 5, pp. 615-623, 1996.

[18] B.D.O. Anderson and J.B. Moore, *Optimal Filtering*, Prentice-Hall, Englewood Cliffs, 1979.

[19] M. Green and D.J.N. Limebeer, *Linear Robust Control*, Prentice-Hall, New Jersey, 1994.

[20] S. Wing, N. Nersessian, and G.P. Carman, Dynamic magnetomechanical behavior of Terfenol-D/Epoxy 1–3 particulate composites, *IEEE Transactions on Magnetics*, Vol. 40, No. 1, 2004.

AKTIVNA KONTROLA VIBRACIJE PRIMJENOM TERFENOLA-D S H-FILTEROM BESKONAČNOG ODZIVA

SAŽETAK

U ovom radu predlaže se materijal s magnetostrikcijom (Terfenol-D) koji se zasniva na aktivnoj kontroli vibracije velike amplitude. Modelira se jedini elastični manipulator planatornog linka s okretnim zglobom koristeći Terfenol-D kao inteligentni aktivni materijal. H-filter s beskonačnim odzivom koristi se u tom kontekstu radi procjene tip-otklona (mjesto) kao i brzine otklona elastičnog manipulatora na kojem se zasniva, a koji se uspoređuje sa shemom aktivne kontrole radi određivanja efikasnosti djelovanja. Zbog derivacije dinamičkog modela slijedi modalni pristup, a zatim se uvodi proporcionalna shema prigušivanja uzimajući u obzir osobine sloja hosta (host layer) i sloja inteligencije (smart layer). Također se govori o izradi kompozitnog aktivatora zasnovanog na Terfenolu-D koji se koristi u eksperimentu. Najprije se obavljaju simulacije koje demonstriraju efektivne sadržaje vibracija i daju potvrdu rezultata koji pokazuju da predložena metoda može efikasno smanjiti vibracije. Međutim, potrebno je optimalno djelovanje kako bi se prepoznali elastični pomaci kao generalizirane koordinate. To se obavlja pomoću diskretizacije elastičnog gibanja kroz pretpostavljenu tehniku moda i primjenom H-filtera s beskonačnim odzivom. H-filter s beskonačnim odzivom se koristi radi usporedbe rada aktivne kontrole vibracija sa shemom prigušivanja. Rezultati simulacija su potvrđeni izvršenim eksperimentima.

***Ključne riječi**: modalna frekvencija, inteligentni kompozitni aktivator, proporcionalno prigušivanje, H-filter s beskonačnim odzivom, Terfenol-D.*